Peculiarities of the height ozone distribution within the transition zone "continent–ocean" by the lidar sensing data

O.A. Bukin, Yu.N. Kul'chin, A.N. Pavlov, S.Yu. Stolyarchuk, and K.A. Shmirko

Institute of Automation and Control Processes,
Far Eastern Branch of Russian Academy of Sciences, Vladivostok

Received April 7, 2008

The results of the atmospheric ozone lidar measurements in transitional "ocean–continent" region in wintertime of 2008 are presented. A concise description of the research equipment is presented as well. The features of the vertical ozone distribution are underlined and a possible explanation of the observed phenomena is suggested based on the trajectory analysis.

Ozone is one of the main active components of the atmosphere, which significantly influences the formation of climatic conditions on the Earth.[1] This influence manifests itself through various mechanisms, the most important of which is the absorption of biologically hazardous short-wave radiation. One more mechanism shows itself in the increase of the difference between atmospheric and stratospheric average temperatures due to variation of the stratospheric ozone concentration. According to some data, in the last decades of the 20th century ozone layer depletion has led to cooling of the upper atmosphere by 3–6°C.[2,3] The stratosphere cooling occurred simultaneously with the increase of amount of the greenhouse gases and a rise of the troposphere temperature. According to estimates of some models,[4,5] the increase of temperature gradients leads to an increase of the wind speed both in stratosphere and at the ground surface.

The recent global climatic models satisfactorily predict such large-scale atmospheric processes in the Southern Hemisphere as circulation of atmospheric upper layers and ozone dynamics over Antarctica. It is believed that Antarctic winds form a relatively stable vortex during the polar night.[6] A complicated topography of the Northern Hemisphere makes arctic atmosphere more dynamic and unpredictable. As well, there is a number of regional peculiarities, which can be taken into account only with more detailed information on spatial (especially altitude) distributional radioactive atmospheric components in hand.

One of these peculiarities is the presence of tropopause discontinuity regions, which significantly influence the processes of exchange between stratosphere and troposphere, as well as atmospheric ozone distribution.[6–9] On the global scale, the study of atmospheric ozone component can be conducted with the help of complex invoking of both satellite and meteorological data, as well as results of lidar sensing of the height ozone distribution (HOD).

The "continent–ocean" transition zone in the north-western part of the Pacific Ocean is a very interesting from the point of view of ozone layer variation specificity. On the one hand, this variation is determined by large-scale continental processes (such as East-Siberian and Asian anticyclones) and, on the other hand, by atmospheric processes over the ocean (e.g. tropical and extra-tropical cyclones).

The strongest ozone layer in the Northern Hemisphere is situated at the latitude of Vladivostok. In 88% of cases it is located over north-east Asia (60–160°E) on the axis of low pressure trough at the level of 100 mbar, which is directed from Indigirka river to Hokkaido island.[9] This planetary maximum is situated to North-East from the core of Siberian winter anticyclone moving along the shore of Japanese, Okhotsk, and Bering Seas. The regional peculiarity of the Asian-Pacific ozone ridge is the behavior of its extremum. Unlike other local maxima of Northern Hemisphere this extremum almost completely disappears in summer period, when the circulation mode changes. On the South this maximum is limited by subtropical zone with frequently repeated jet streams at its borders flowing over Japan from the West to the North-East.[10,17] These jet streams play an important role in the exchange process between stratosphere and troposphere in tropopause discontinuity zone near the stream axis.[11,12]

Besides, tropical cyclones, typical for this region, lead to HOD change as well. The authors of Ref. 13 present the results, demonstrating that in the majority of tropical cyclones the troposphere ozone content decreases (66% for developing tropical depression; 72% for tropical storm) and stratosphere ozone concentration increases. As for the tropical storms (TS) and typhoons (TY) a decrease of ozone concentration in both troposphere and stratosphere is observed in 51% cases. This is connected with intrusion of rising flows with TS and TY to high altitudes.

The specifics of this region are conditioned by its proximity to the main supplier of aerosol into the atmosphere, i.e., the Gobi Desert, which has a strong influence on the dynamics of radiation-active

0235-6880/08/10 769-06 $02.00

components of the atmosphere. Its proximity to arid land regions shows itself from February to June, when the leading Asian anticyclone transports the continental aerosol to the altitude of tropopause,[14] actively interacting with ozone and such additionally decreasing its concentration.[6,9,15]

In order to investigate the HOD dynamics in "continent–ocean" transition zone at the Gulf of Peter the Great shore (IACP FEB RAS lidar station, 43.2°N, 131.9°E), the ozone lidar was installed, developed at the Center of Physical Instrument Engineering of A.M. Prokhorov Institute of General Physics. The lidar allows measuring the HOD in the altitude range between 1 and 45 km, as well as water vapor within 0.6–3 km. As well, there is a channel for measuring the intensity of Raman scattering of the atmospheric nitrogen.

The set specifications are the following: a 600 mm surface telescope aperture, the XeCl-laser CL7000 as a radiation source, a 308 nm wavelength of the eximer laser radiation, a 270 mJ energy in a pulse, a 100 Hz pulse repetition rate. A hydrogen cell was used for SR transformation of the laser radiation frequency into 335 nm radiation. The recording system operates in photon counting mode via 8 channels with Hamamatsu R7400 photoelectric multiplier. To narrow the dynamic range of the recorded signal, mechanical and electronic cutoffs are used, capable of working both in joined and separate modes. Minimal altitude for the effective signal cutoff is approximately 6 km.

To retrieve the ozone vertical distribution in the atmosphere from the sensing data, the method of differential absorption, based on different ways of optical radiation attenuation at close wavelengths, is used.[16]

The ozone concentration is calculated by the formula

$$n_{oz} = -\frac{1}{2\Delta\sigma_{oz}}\frac{\partial}{\partial z}\ln\left(\frac{P_{on}}{P_{off}}\right) - \frac{1}{\Delta\sigma_{oz}}(\alpha^R_{on} - \alpha^R_{off}),$$

where $\Delta\sigma_{oz} = \sigma^{on}_{oz} - \sigma^{off}_{oz}$ is the differential cross section of the ozone absorption; P_{on}, P_{off} are scattered radiation intensities at two wavelengths; α^R corresponds to the molecular attenuation at the corresponding wavelengths; indices "on" and "off" correspond to 308 and 353 nm wavelengths, respectively.

To calculate the profiles of molecular attenuation and backscattering, the data of meteorological sensing of temperature were used. The sensing was performed two times a day (at 00.00 and 12.00 UTC)[17] in the vicinity of the lidar station. This allowed us to account for regional and seasonal peculiarities, which showed themselves at altitude temperature distribution.

Since the differential absorption method is sensitive to the magnitude of ratio of the backscattering signal to noise, then when retrieving the ozone concentration profile, the adaptive polynomial filter of the second order in a sliding window was used. This approach allows obtaining simultaneously both the smoothed backscattering signal value and its derivative in each measured points.

For each point *X*, a window, containing *n* points to the left and to the write from the initial one, was chosen. Using the least square method, the selected set of points was approximated by second degree polynomial and then the smoothed continuous functions of a signal and the derivative were used in calculation of the ozone concentration. The main peculiarity of this method is the dynamic variation of the smoothing window in the set limits in accordance with variation of dispersion of the signal values in the selected point.

As a result of HOD measurements, conducted from June, 2007, the registration of two types of distribution was noted. The first of them is characterized by the presence of one maximum at an altitude range of about 20 km, while the second type, which occurs more often in winter period has several local maxima (the stratified HOD structure). Ozone concentration profiles in the presence and in the absence of complex HOD structure (according to lidar measurements) in January–March, 2008 are presented in Fig. 1*a*. The HOD maximum for this period is located at 20 km altitude with distribution of half-width of 15 km within 12–27 km region. Maximal concentration reaches $5\cdot10^{12}$ mol.$\cdot$cm^{-3}, which corresponds to the values determined for these latitudes.[9]

In winter period the possibility of appearance of the local HOD maximum at 12–15 km altitude is more than 80%.

To find most dynamic region on the profile, we constructed a profile of standard deviation, presented in Fig. 1*b*. As is seen, the maximal HOD dispersion corresponds to the altitude range with minimum ozone distribution, i.e., to ~14 km. However, we can not exactly state that just at this layer is a decrease in ozone concentration.

We should note that dynamic processes, conditioned by the influence of polar vortex mostly show themselves at the lower (left) wing of the HOD, while the upper (right) part remains relatively stable. The increase of the HOD dispersion in winter period of 2008 (not significant) was marked even at an altitude of 35 km, which, most probably was related to periodic transfer of air masses from the South with tropical type of HOD.

The stratified structure of midlatitude ozone profiles was first described in Ref. 18. Such anomalous profiles are typical for European moderate latitudes, especially in cyclonic conditions of spring and winter.[19] They are typical for polar air masses in moderate latitudes (according to Hrgian classification[9]). This type is rarer in subtropical and anticyclonic situations. First climatology of a stratified structure, based on satellite and lidar data, was presented in Ref. 20. Stratified structure formalization was proposed in Refs. 9 and 21. The HOD local maximum within 12–15 km range was defined as a second maximum in Ref. 21.

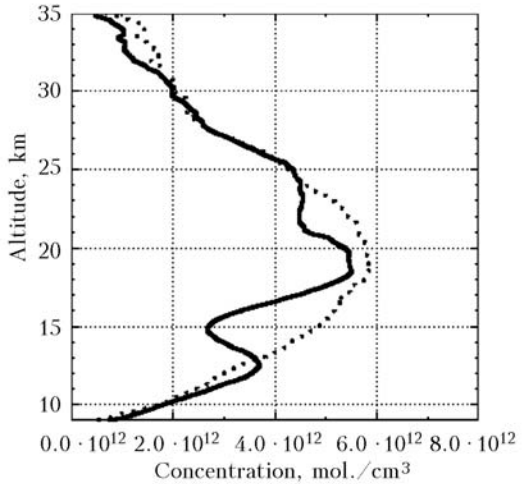

a

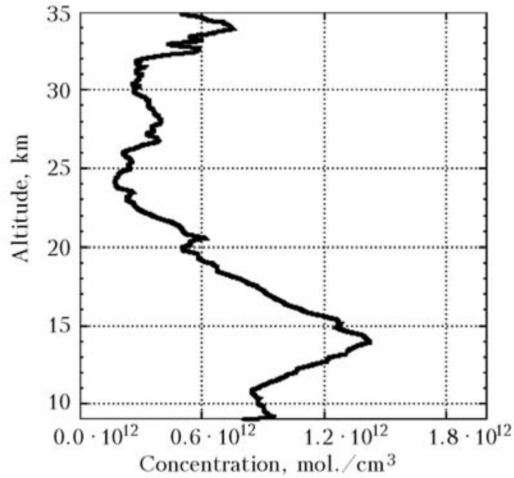

b

Fig. 1. Vertical profiles of ozone concentration distribution for 01.22.2008 (solid line) and for 01.25.2008 (dot line) (*a*); root-mean-square deviation of ozone concentration deviation according to the altitude for January–February, 2006 (*b*).

The following processes lead to formation of the HOD stratified structure[22,23]: 1) transport of air chemical mixture of winter polar vortex, ready to photochemical ozone destruction in sunlight, which leads to ozone destruction at moderate latitudes; 2) transport of polar vortex air masses with destructed ozone to moderate latitudes, leading to the stratified structure; 3) transport of tropical air masses with low ozone content, leading to ozone content lowering in stratosphere of high latitudes and the intrusion to the vortex periphery; 4) transport of ozone-rich arctic air to stratosphere moderate latitudes.

We can point out two main factors, which influence total content and structure of HOD in our region: polar vortex periphery destruction and the position of jet stream, which stipulates significant gradients of TOC near its northern border. According to the model data of Ref. 11, based on many-year analysis, maximal possibility of the presence of air mass streams, separated from the polar vortex, is observed at the Pacific coast. A possible distribution of jet streams on the global scale is presented in Ref. 11. One of them, subtropical, runs in parallel to the equator at 20–25°N, originating in the region of zero meridian. Having reached 120°E, it changes its direction to the North pole in such a way that its trajectory runs in close proximity to the lidar station through Japan Archipelago, Kamchatka, and the Kuril Islands. This stream is a kind of barrier which traps the air masses of Arctic polar vortex over north-west waters of the Pacific Ocean.

To determine the sources of the observed distributions and the nature of the secondary peak in ozone distribution over lidar station site, the trajectory of the air mass movement[24] has been analyzed for altitudes, corresponding to the secondary and main maxima of ozone distribution, as well as to the minimum, separating them. The authors of Ref. 25 supposed that the secondary maximum is conditioned by the northern air masses, enriched with ozone. The inverse trajectory analysis allows us to retrieve the trajectory of air mass movement before the moment of reaching the lidar station and estimate the time of ozone tracer presence at different latitudes. To generalize the results of trajectory analysis and the validity of the suggestion[25] for our region, histograms of the inverse trajectory analysis were built.

Figure 2 illustrates trajectory (*a*) and histogram (*b*–*d*) analyses of HOD, presented for January 22 in Fig. 1*a*.

Circles in Fig. 2 indicate the trajectory of particles for the altitude corresponding to the secondary maximum, triangles indicate the trajectory of particles at the altitude, separating the main and secondary maxima; squares denote the trajectory of particles corresponding to the altitude of the main maximum. According to the obtained movement trajectories for January 22, the source of air masses at the altitude of the secondary maximum and minimum above the lidar station is a polar vortex, while the main HOD maximum is caused by the injection of subtropical air masses. This situation was characteristic of January and February. For comparison, the same analysis was conducted for 01.25.2008. The HOD profile this day did not have any peculiarities. The trajectory analysis has shown a difference, which is in the fact that particle trajectories were separated in space most time and had joint points only in the beginning and the end of the analyzed period (on 01.22.2008, particle trajectories almost coincided in the end of the movement, and each trajectory had its own beginning). Note that closer to the lidar station particles trajectories overlapped the jet stream.

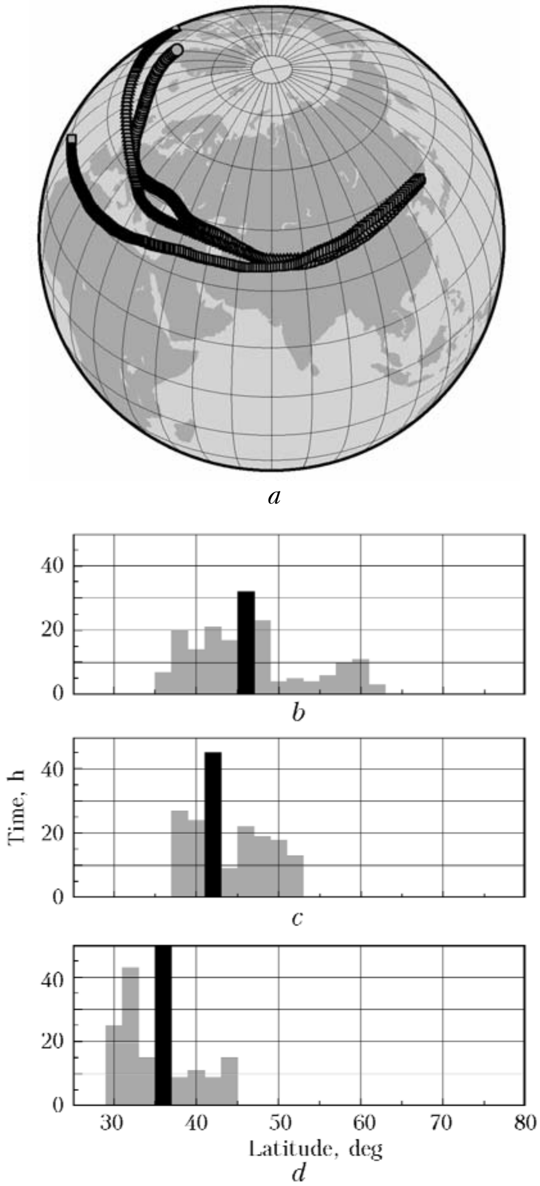

Fig. 2. Trajectory analysis of air mass movement for 01.22.08 (*a*); histogram analysis of air mass movement for different horizons of 01.22.08 (*b–d*): ● is the altitude of secondary maximum; ▲ is the altitude of minimum; ■ is the altitude of main maximum.

Figures 2*b–d* allow a conclusion that maximal time and, consequently, the probability of locating particle to the altitude of the secondary maximum were shifted to the direction of northern latitudes relative to the probability of their presence at the altitude of the main maximum. The comparison with 01.25.2008 has revealed that most possible latitudes for each level were shifted 01.22.2008 to the South.

Trajectory analysis with constructing similar histograms was conducted also for neighboring areas from Sakhalin to Kamchatka, where, according to satellite data, the absolute maximum of ozone content that time was located. Even though up to altitude of more than 20 km the transport originates mainly from polar regions (with insignificant differences some days), the observed difference in the ozone total content can be explained by significant differences in transport speed and the time of residence of certain air masses at low latitudes in the process of their transport.

Polar air masses came to the region of local absolute maximum by shorter paths and, consequently, sooner. However, they arrived to the region of lidar station mainly due to long-term transport of polar filaments caught by the periphery of subtropical jet stream. After polar streams left the night zone, the influence of solar radiation caused photochemical ozone destruction in the presence of chemical reagents accumulated in polar vortex for the long period of light absence. This process causes the ozone depletion at altitudes of 15–16 km (see Fig. 1), typical for altitude distribution in polar vortex in spring period, when photochemical process of ozone destruction in the presence of NO_x occurs.[26]

Ozone layer depletion can be also caused by its proximity to the jet stream. Particle flow speed in the center of jet stream is about 120 knots decreasing down to 50–60 knots at the periphery. As it was mentioned in Ref. 27, the possibility of the presence of peculiarities in HOD decreased as the center of jet stream moved away from the observation site.

In the preliminary analysis of obtained HOD structure the HOD were divided into two similar groups. The HOD with local maxima conditioned by direct invasion of polar filaments fell in the first group. This invasion was proved by inverse trajectory analysis and by the analysis of potential vortex maps obtained in the framework of MIMOSA model.[26] The HOD with local maxima, caused by ozone concentration decrease at altitudes of 15 km relative to average distribution, fell in the second group.

To estimate the interrelation of HOD parameters with ozone total content in winter period of 2007/08, time dependences of ozone integral content (Fig. 3*a*), positions of the main and secondary maxima (Fig. 3*b*), and HOD center of gravity (Fig. 3*c*) were built.

We should note that TOC was calculated for the ozone layer between 9 and 35 km and the obtained values are lower than those obtained by other methods (satellite scanners, radiometers, Dobson spectrometers). However, they are in good agreement with TOC data from Ref. 9.

For the obtained time series (position of center of gravity, main maximum and TOC) the correlation coefficient was calculated.

A good anticorrelation between the altitude of center of gravity and TOC is observed (–0.9). The correlation coefficient between TOC and position of main maximum is –0.86. This fact well agrees with results of many-year observations, according to which the TOC has a tendency to increase from the beginning of spring until April. Linear dependence between the position of the main HOD maximum and tropopause altitude was also revealed.[28] The tropopause altitude is characterized by seasonal variations, which are reflected in the position of HOD maximum. According to our data, when the distance to regional maximum decreased, the observed HOD on the whole changed in such a way that altitude positions of secondary and main maxima decreased with the TOC increase.

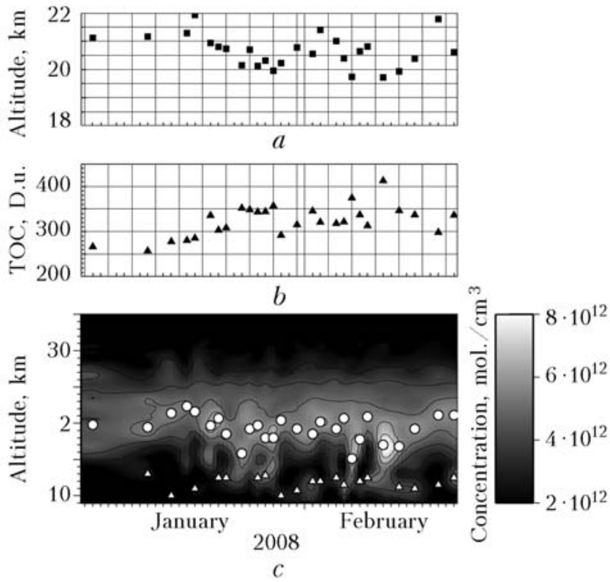

Fig. 3. Altitude of HOD center of gravity (*a*); time behavior of TOC (*b*); HOD time development (shade of gray) with marked positions of the main (circles) and secondary (triangles) maxima (*c*).

The lidar sensing revealed a complex HOD structure in "continent–ocean" transition zone at the lidar location site. Basing on the joint analysis of the obtained HOD, air mass trajectories, and potential vortex maps, it can be supposed that the lower secondary maximum at the level of tropopause is, in most cases, caused by the invasion of arctic air masses to below the axis of the jet stream. However, the observed stratified structure is quite stable in winter period and also might be caused by ozone concentration decrease in the lower stratosphere in the process of ozone transport from polar vortex to the South, as well as by its movement in the process of trapping by the jet stream. During the observed period the position of the center of this jet stream in our region has changed within 10°. It was revealed that for the HOD of all types the general increase of ozone content anti-correlates with the altitude of the main maximum and the center of gravity of ozone layer distribution.

Significant variability of HOD structure reflects seasonal dynamics of atmospheric processes at the investigated altitudes at the "continent–ocean" transition zone of the north-western part of the Pacific Ocean. This variability is caused by interaction of air masses, mixing under the influence of polar vortex and jet streams, parameters of which in their turn have not only a significant seasonal variability, but are also determined by common planetary climatic changes.

Acknowledgements

The authors are grateful to I.A. Veselovskii for his help in adjusting and actuating equipment, as well as to V.V. Zuev for fruitful discussions of ozone lidar sensing data.

This work was financially supported by Russian Foundation for Basic Research (Grant No. 07-05-13505); FEB RAS (Grants Nos. 06-I-P16-060, 06-II-CO-07-028), and Federal Agency on Science and Innovations State (Contract No. 02.518.11.7064).

References

1. D.T. Shindell, G. Faluvegi, A. Lacis, J. Hansen, R. Ruedy, and E. Aguilar, J. Geophys. Res. D 08302, doi:10.1029/2005JD006348 (2006).
2. D.T. Shindell, Geophys. Res. Lett. **28**, No. 8, 1551–1554 (2001).
3. A.A. Chernikov and A.A. Kivolutskiy, National report: National geophysical committee Russian Academy of Sciences to the International Association of Meteorology and Atmospheric Sciences of the International Union of GeHODesy and Geophysics 1995–1998, http://www.wdcb.ru/NGC/IAMAS.html
4. D.T. Shindell, Science, doi:10.1126/science.1080855 (2003).
5. D.T. Shindell, Geophys. Res. Lett. **34**. doi:10.1029/2007GL030221 (2007).
6. Center for Coastal Physical Oceanography, www.ccpo.HODu.edu
7. H.M. Fischer, C. Birk, B. Blom, B.Carli, M. Carlotti, von T. Clarmann, L. Delbouille, A. Dudhia, D. Ehhalt, M. Endemann, J.-M. Flaud, R. Gessner, A. Kleinert, R. Koopmann, J. Langen, M. López-Puertas, P. Mosner, H. Nett, H. Oelhaf, G. Perron, J. Remedios, M. Ridolfi, G. Stiller, and R. Zander, Atmos. Chem. Phys. Discuss. **7**, 8795–8893 (2007).
8. J. Hansen, J. Geophys. Res. **110**, D18104, doi:10.1029/2005JD005776 (2005).
9. A.Kh. Khrgian, *Atmospheric Ozone Physics* (Gidrometeoizdat, Leningrad, 1973), 290 pp.
10. T. Nagahama, in: *Proc. of the 4 Int. Workshop on Global Change: Connection to the Arctic*, Toyokawa, Aichi, Japan (2003), pp. 170–174.
11. K. Krüger, U. Langematz, J.L. Grenfell, and K. Labitzke, Atmos. Chem. Phys., Iss. 5, 547–562 (2005).
12. G. Vaughan, F.M. O'Connor, and D.P. Warein, J. Atmos. Chem. **38**, No. 3, 295–315 (2001).
13. A.F. Nerushev, *The Influence of Strong Atmospheric Vortexs on the Ozone Layer* (Saint-Petersburg, Gidrometeoizdat, 2003), 223 pp.
14. O.A. Bukin, A.N. Pavlov, P.A. Salyuk, et al. Atmos. Oceanic Opt. **20**, No. 4, 306–312 (2007).
15. V.V. Zuev, A.V. El'nikov, and V.D. Burlakov, *Middle Atmosphere Laser Sensing* (Rasco, Tomsk, 2002), 280 pp.
16. I. Veselovskii and B. Barchunov, Appl. Phys. **68**, No. 6, 1131–1137 (1999).
17. Atmospheric Soundings, http://weather.uwyo.edu/upperair/sounding.html
18. G.M.B. Dobson, Appl. Geophys. **106–108**, Nos. 5–7, 1520–1530 (1973).
19. S.J. Reid and G. Vaughan, Quart. J. Roy Meteorol. Soc. **117**, Iss. 500, 825–844 (1991).

20. C. Appenzeller and J.R. Holton, J. Geophys. Res. D **102**, No. 12, 13555–13569 (1997).
21. P. Krizan and J. Lastovicka, Stud. Geophys. Geod. **48**, No. 4, 777–789 (2004).
22. S. Balestri, D. Balis, and T. Blumenstock, *The Northen Hemisphere Stratosphere in the 2002/03 winter: Preliminary Results from the first phase of VINTERSOL* (University of Cambridge, 2004), 34 pp.
23. D. Balis, T. Blumenstock, and M.P. Chipperfield, *The Northern Hemisphere Stratosphere in the 2006/07 Winter: preliminary results provided by European and collaborating scientists* (University of Cambridge, 2007), 17 pp.
24. Air Research Laboratory, www.arl.noaa.gov
25. R. Lemoine, Atmos. Phys. Chem. Discuss., No. 4, 1791–1816 (2004).
26. A. Hauchecorne, S. Ghodin, M. Marchand, and B. Heese, J. Geophys. Res. **107**, No. 20, 8289–8302 (2002), 8229, doi:10.1029/2001JD000491, 2002.
27. G.O. Braathen, *Ozone and Aerosol Zond Activities*: Report to NDSC Steering committee (Norwegian Institute for air researches, Thun, 2003), 34 pp.
28. L.T. Matveev, *Course of General Meteorology. Atmospheric Physics* (Gidrometeoizdat, Leningrad, 1984), 725 pp.